

Influence of Low Oxygen Tensions and Sorption to Sediment Black Carbon on Biodegradation of Pyrene[∇]

José-Julio Ortega-Calvo^{1,2*} and Philip M. Gschwend²

*Instituto de Recursos Naturales y Agrobiología (IRNAS), C.S.I.C., Apartado 1052, E-41080 Seville, Spain,¹ and
Ralph M. Parsons Laboratory, MIT 48-415, Department of Civil and Environmental Engineering,
Massachusetts Institute of Technology, Cambridge, Massachusetts 02139²*

Received 20 February 2010/Accepted 6 May 2010

Sorption to sediment black carbon (BC) may limit the aerobic biodegradation of polycyclic aromatic hydrocarbons (PAHs) in resuspension events and intact sediment beds. We examined this hypothesis experimentally under conditions that were realistic in terms of oxygen concentrations and BC content. A new method, based on synchronous fluorescence observations of ¹⁴C-pyrene, was developed for continuously measuring the uptake of dissolved pyrene by *Mycobacterium gilvum* VM552, a representative degrader of PAHs. The effect of oxygen and pyrene concentrations on pyrene uptake followed Michaelis-Menten kinetics, resulting in a dissolved oxygen half-saturation constant (K_{om}) of 14.1 μ M and a dissolved pyrene half-saturation constant (K_{pm}) of 6 nM. The fluorescence of ¹⁴C-pyrene in air-saturated suspensions of sediments and induced cells followed time courses that reflected simultaneous desorption and biodegradation of pyrene, ultimately causing a quasi-steady-state concentration of dissolved pyrene balancing desorptive inputs and biodegradation removals. The increasing concentrations of ¹⁴CO₂ in these suspensions, as determined with liquid scintillation, evidenced the strong impact of sorption to BC-rich sediments on the biodegradation rate. Using the best-fit parameter values, we integrated oxygen and sorption effects and showed that oxygen tensions far below saturation levels in water are sufficient to enable significant decreases in the steady-state concentrations of aqueous-phase pyrene. These findings may be relevant for bioaccumulation scenarios that consider the effect of sediment resuspension events on exposure to water column and sediment pore water, as well as the direct uptake of PAHs from sediments.

The aerobic biodegradation of polycyclic aromatic hydrocarbons (PAHs) constitutes one of the main processes for dissipation of these toxic compounds from polluted soils and sediments. The oxygen dependence of this process has long sustained the belief that the anaerobic conditions usually found in environments such as sediments in estuaries and ports are the main cause of a long persistence of PAH pollution. However, recent findings have demonstrated that microorganisms can also use other electron acceptors, such as nitrate and sulfate, to oxidize PAHs in sediments (30, 33). Less attention has been given to aerobic biodegradation operating at low oxygen tensions. This process may also be important at the interface between anoxic sediments and the overlying waters. Resuspension of PAH-polluted anoxic sediments can result in the exposure of sediment particles to low concentrations of oxygen in the immediately overlying water column, thereby promoting the aerobic biodegradation of PAHs (22) under conditions in which they can be desorbed and taken up by competent microorganisms. The resulting decreases in the aqueous-phase concentration (and in the associated chemical activity) caused by oxygen-limited aerobic biodegradation may be relevant for bioaccumulation scenarios that consider exposure to the water column and sediment pore water, in addition to the direct uptake from sediments (23). Despite its signifi-

cance, the capacity for prediction of aerobic biodegradation rates of PAHs at low oxygen tensions is still very limited. Whereas the oxygen dependence of fast biodegradation of PAHs in soils and sediments is a well-known phenomenon (5, 17), studies reporting precise measurements of the dissolved oxygen half-saturation constant (K_{om}) for biodegradation of PAHs—a key modeling parameter—are very scarce (7, 21). The only available estimation for a K_{om} value of a high-molecular-weight (HMW) PAH (5.9 μ M) was provided for pyrene on the basis of growth rates on pyrene of a *Mycobacterium* strain in a fermenter (7). However, the pyrene concentration chosen (500 mg/liter)—well above the level of its aqueous solubility (0.13 mg/liter) known to support bacterial growth (34)—was not representative of those concentrations present in the environment.

Besides the oxygen concentration, another factor that may control the biodegradation of sedimentary PAHs is their bioavailability. Due to their partitioning into sorbents, such chemicals exhibit only weak chemical activity gradients that promote their uptake and transformation by active microbial cells. Hence, the biodegradation rates are likely far below those corresponding to maximum rates, and they may reflect nonlinear biochemical dependencies. Also, these low rates may be due to the lower chemical activity of PAHs causing the microbial acquisition of the aqueous-phase chemicals to become a bottleneck for the biodegradation process (31). Examples of conflicts of bioavailability with biodegradation can be found when PAHs are predominantly sorbed onto solid aggregates (12) and dissolved in non-aqueous-phase liquids (28). Sorption is especially important

* Corresponding author. Mailing address: Instituto de Recursos Naturales y Agrobiología (IRNAS), C.S.I.C., Apartado 1052, E-41080 Seville, Spain. Phone: 34 95 4624711. Fax: 34 95 4624002. E-mail: jjortega@irnase.csic.es.

[∇] Published ahead of print on 14 May 2010.

in sediments. During recent years, the traditional, one-phase organic carbon (OC) partitioning model has been expanded for PAHs and other hydrophobic pollutants to include uptake both into OC and onto the ubiquitous, solid-phase products of incomplete combustion, collectively called black carbon (BC). Therefore, adsorption to BC and absorption to OC would occur in parallel during the sorption process (1, 2, 15). The new model has been useful in understanding field observations of the PAH solid-water distribution coefficient (K_d), which have evidenced a higher sorption capacity than would have been expected on the basis of OC content only (25, 26). Several studies have shown that strong sorption of PAHs to BC may also significantly limit biodegradation. For example, Ghosh et al. showed that 16 U.S. Environmental Protection Agency (USEPA) PAHs associated with carbonaceous coal-derived material present in harbor sediments exhibited negligible biodegradation rates in aerobic sediment slurries, whereas similar conditions led to significant losses (up to 75% after 2 months) of PAHs present in semisolid coal tar pitch (10). Little or no biodegradation was also observed for 3- to 6-ringed PAHs associated with BC-rich street dust added to soils to simulate diffuse pollution (18) and with naphthalene sorbed to granular activated carbon, a material similar to BC in its physicochemical characteristics, in suspensions of two different bacterial species with dissimilar modes of acquisition of the sorbed compound (14). Finally, Rhodes et al. examined the effect of BC on bioavailability of phenanthrene in soils (32). They found that the addition of BC to soils caused a significant decrease both in the total extent of mineralization and in extractability by the use of cyclodextrin solutions (32). Despite these advances in the field, it is still uncertain whether sorption to BC causes the sequestration of PAHs or whether their microbial assimilation is still possible, although at a very low rate. This gap in knowledge is a major limitation in predicting the fate of these chemicals in many contaminated sediments, making it difficult to achieve a proper perception of the risks posed by resuspensions in overlying waters and bioturbated sediment beds.

We considered that sorption to sediment BC may limit the aerobic biodegradation of aqueous-phase PAHs such as pyrene and examined this hypothesis experimentally under conditions that were realistic in terms of concentrations of oxygen and suspended-solids typical for sediment resuspension events. For this aim, we developed a new method, based on synchronous fluorescence observations of ^{14}C -pyrene, for both measuring the rates of uptake of dissolved pyrene at low oxygen concentrations by a representative PAH-degrading bacterial strain and simultaneously assessing the appearance of $^{14}\text{CO}_2$. The method also allowed us to characterize the evolution of aqueous-phase pyrene during biodegradation in initially equilibrated suspensions of sediment with a known content in black carbon. The information obtained experimentally was integrated in model calculations of the evolution of aqueous pyrene concentrations in sediment suspensions. To our knowledge, this is the first report connecting these two major factors—oxygen limitation and sorption to BC—in the biodegradation of HMW PAHs.

MATERIALS AND METHODS

Chemicals. [$4,5,9,10\text{-}^{14}\text{C}$]Pyrene (55 mCi/mmol; radiochemical purity, >97%) was obtained from Sigma-Aldrich, Saint Louis, MO. Nonlabeled pyrene (purity, 99%) was purchased from Aldrich Chemical Co., Milwaukee, WI.

Bacterium, media, and cultivation. *Mycobacterium gilvum* VM552 was used, because it can grow with pyrene as the sole source of carbon and energy. Bacteria of the genus *Mycobacterium* have previously been identified as representative components of PAH-degrading populations in Boston Harbor sediments (4). The strain, which was kindly supplied by D. Springael (Catholic University of Leuven, Leuven, Belgium), was grown exponentially at 30°C in a phosphate-buffered solid medium (pH 7.0) described previously (35). Pyrene had earlier been added to the sterile medium at 45°C in acetone solution (0.033 g/ml) to give a final concentration of 0.10 g/liter. This temperature facilitated the fast evaporation of the acetone prior use of the plates. This procedure resulted in the formation of fine crystals whose dissolution through the agar allowed the growth of *M. gilvum*. Noninduced cells were obtained after growth on solid Luria broth (LB) medium (35). For biodegradation experiments, early-stationary-phase cells were collected 2 weeks (pyrene) or a few days (LB) after inoculation, by a washing of the surface of the agar with pyrene-free medium, centrifugation at $1,700 \times g$ for 20 min, and a further single washing performed once with the same medium. Final cell densities were adjusted by measurement of the optical density at 600 nm (OD_{600}) as stated below. The medium, which was also used in all biodegradation experiments, was prepared as described above and previously (35), except that the concentrations of $\text{K}_2\text{HPO}_4 \cdot 3\text{H}_2\text{O}$ and $\text{NaH}_2\text{PO}_4 \cdot 3\text{H}_2\text{O}$ were 0.65 and 3.70 g/liter, respectively, and were buffered to pH 5.8.

Sediment. The sediment sample used in this study was obtained from North Quincy Bay (NQB) in Boston Harbor, a site with a known record of pollution by PAH. The sediment has been studied in terms of chemical composition and sorption capacity for PAHs (1, 24). It has 3.1% organic matter, 0.6% black carbon, and approximately 11 mg of pyrene/kg of dry sediment. The sediment sample was prepared for the experiments as described earlier (1). For some experiments, NQB sediment was enriched with black carbon by mixing (1% [wt/wt]) with diesel particulate matter (SRM 2975; National Institute of Standards and Technology, Gaithersburg, MD) (0.9 mg of pyrene/kg of dry matter). This sample is referred to here as NQB-BC. The sediment samples were left unsterilized to avoid alteration of their sorption capacity, but sorption controls (see below) evidenced no pyrene biodegradation activity in the absence of inoculation.

Sorption. Sediment samples (20 to 80 mg) were introduced into 60-ml BOD glass bottles (Wheaton), together with 50 ml of distilled water containing 8.4 ng/ml dissolved ^{14}C -pyrene (5,000 dpm/ml). The resulting range of concentrations of suspended solids (400 to 1,600 mg solids/liter) can be considered realistic for natural estuary, harbor, or tributary water columns, which typically contain 20 to 500 mg of solids/liter (20), and for waters receiving inputs of solids (130 to 2,300 mg solids/liter) during resuspensions of PAH-polluted sediments (37). The radiolabeled compound had been added to the aqueous solution dissolved in acetone (0.1 ml acetone per liter of water). This acetone concentration was low enough to cause a cosolvent effect or toxicity for the bacteria. The bottles were closed with glass stoppers and tumbled once every 17 s for 200 h. This sorption equilibration period was sufficient to cause restrictions for biodegradation of sediment-sorbed PAH (12).

The concentration of ^{14}C -pyrene in solution was determined by synchronous fluorescence analysis (36) of homogenous samples taken from the flasks and transferred to a quartz cuvette (model 13LT PCS2; NSG Precision Cells, Inc., Farmingdale, NY) (1-cm path length). The scans were performed using a Perkin-Elmer LS50B luminescence spectrofluorometer (Buckinghamshire, England), with a $\Delta\lambda$ of 100 nm (i.e., quantifying response with excitation at 272.4 nm and emission at 372.4 nm), an entrance slit width of 2.5 nm, an exit slit width of 5 nm, and a scan speed of 240 nm/min. The detection limit with these parameters was 0.27 ng of pyrene/ml (1). The specific activity of ^{14}C -labeled pyrene was calculated from the calibration with solutions of ^{12}C -pyrene in water and independent measurement of radioactivity with a liquid scintillation counter (model LS6500; Beckman Instruments). We found that the specific activity was $94.9 \pm 4.2\%$ of the value stated by the supplier. Inner-filter effects on the fluorescence quantifications in sediment suspensions were corrected for each determination according to the method of Gauthier et al. (8), using measurements of absorbance at 272.4 nm and 372.4 nm obtained with a Beckman DU640 spectrophotometer (Fullerton, CA). The correction factors ($F_{\text{corr}}/F_{\text{obsd}}$) were calculated from absorbance readings taken after 5 min, a period within which most of the bigger particles had settled. Settling did not interfere during fluorescence measurements, since the fluorescence remained constant (at <9% of the initial fluorescence values) over at least the first 20 min. Correction factors typically ranged from 1.03 to 1.18. The accuracy of these corrections was also confirmed by the

limited (<1%) deviation of the values calculated from fluorescence determinations for pyrene in supernatants of the samples after centrifugation at 1,700 × *g* for 20 min. Fluorescence readings taken during 20 min for a solution of pyrene (8.2 ng/ml) in culture medium confirmed that sorption of the chemical to the walls of the fluorimeter cuvette was below the instrumental error level (6.5%). Losses of dissolved ¹⁴C-pyrene in control bottles without sediment were <4% during the experiment. No mineralization occurred in the sediment suspensions during equilibration, as indicated by the absence of detectable ¹⁴CO₂ in the solution. Interference caused by the presence of native pyrene in fluorescence determinations was not observed, even though the pyrene contribution in the sediment was between half and twice the ¹⁴C-pyrene spiking level, as we saw that sediment suspensions maintained under the same conditions, but without added ¹⁴C-pyrene, had no pyrene fluorescence signal. The solid-water distribution coefficient, *K_d* (in liters per kilogram), was calculated from the following equation:

$$f_w = \frac{1}{1 + r_{sw}K_d} \quad (1)$$

where *f_w* is the fraction of the compound remaining dissolved in the water at equilibrium and *r_{sw}* is the solid-water phase ratio in kilograms per liter.

Biodegradation. Experiments were performed at 23°C using the fluorimeter cuvette under conditions that allowed us to follow continuously the disappearance of pyrene from the aqueous solution. This was achieved by taking advantage of the higher specificity of the signal from pyrene observed with synchronous spectrofluorometry compared with conventional fluorimetry. The synchronous method uses a fixed Δλ (emission minus excitation) during the scan that helps discriminate target fluorophores (e.g., pyrene) from interfering signals from sediment, bacterial cells, and inorganic salts present in the culture medium. The experiments included (i) biodegradation in sediment-free media at different oxygen concentrations and (ii) biodegradation in air-saturated sediment suspensions.

The effects of different oxygen concentrations on biodegradation were tested using bacterial suspensions prepared in the fluorimeter cuvette by mixing known volumes of oxygen-free and air-saturated bacterial suspensions and ¹⁴C-pyrene solutions. The mixtures were prepared in a nitrogen atmosphere inside a glove bag provided with an oxygen trap in the inlet (VWR, Batavia, IL). Oxygen-free and air-saturated suspensions were prepared by sparging with nitrogen and air, respectively, for 3 min. The concentration of oxygen in the cuvette was calculated from the oxygen concentration in air-saturated culture medium (8.4 mg/liter or 262.5 μM at 23°C, as measured with a model 57 oxygen meter provided with a 5905 BOD probe [YSI, Yellow Springs, OH]) and from the volumes of the different oxic and anoxic solutions used in the reaction. The absence of detectable amounts of oxygen in nitrogen-sparged suspensions was confirmed with oxygen meter and colorimetric determinations (Chemets kit R-7501; Chemetrics, Calverton, VA) (limit of detection, 0.05 mg/liter or 1.6 μM). The cuvette was then immediately sealed with a ground glass stopper and transferred from the glove bag directly into the fluorimeter. The concentration of pyrene in solution was then measured in all of the experiments every 30 s by synchronous scans performed as previously described, using appropriate corrections for inner-filter effects. Experiments with killed bacteria were performed by adding, at 5 min prior to experiments, 50 μl of a solution of HgCl₂ (40 g/liter) to 4 ml of the bacterial suspensions.

Because the fluorescence calibrations at low oxygen tensions had a higher slope than in air-saturated solutions (thus evidencing the quenching effect of oxygen on fluorescence), a separate calibration was used for each oxygen concentration tested. For example, calibration at 13 μM oxygen followed the relationship $y = 20.63 \times -1.48$ ($R^2 = 0.98$), whereas, for air-saturated solutions (262.5 μM oxygen), calibration followed the equation $y = 15.25 \times -7.19$ ($R^2 = 0.98$). Because of the nanomolar-range concentrations of pyrene used and the stoichiometry of the aerobic oxidation of this compound, significant changes in the concentration of oxygen due to biodegradation were not expected. Although the suspensions were not stirred, the bacterial cells remained homogeneously suspended during the experiments, as revealed by independent absorbance measurements performed at 272.4 nm and 600 nm during 1 h.

The effect of sorption on pyrene biodegradation was tested under fully aerated conditions in aliquots of sediment suspensions equilibrated as described above for the sorption experiments. Again, considering the experimental period used, the low concentration of organic-matter-containing solids present, and the use of pyrene-induced cells, no significant oxygen limitation was expected. To measure biodegradation, 4-ml portions of the sediment suspensions were placed in the fluorimeter cuvette, supplemented with 100 μl of a 40-fold-concentrated mineral medium (pH 5.8), and inoculated with 75 μl of a bacterial suspension prepared as described above. The fluorescence signal of pyrene was then monitored by synchronous scans.

The fluorescence signal of ¹⁴C-pyrene could not be identified in bacterial suspensions having an OD₆₀₀ higher than 0.03. Therefore, the cell density in the assay mixtures was adjusted (unless otherwise stated) to an OD₆₀₀ of 0.010 ± 0.003. In experiments with sediment suspensions, cell densities were adjusted in parallel by measuring the OD₆₀₀ of bacterial suspensions at appropriate dilutions in sediment-free medium. The protein concentrations in the assay mixtures were estimated for each experiment (6), with bovine serum albumin (Sigma-Aldrich, Saint Louis, MO) as the standard. A cell suspension with an OD₆₀₀ of 0.007 had a protein content of 2.81 μg/ml and 2 × 10⁹ cells/ml. The cell densities used were slightly higher than those usually found in natural sediments and pore waters (see Results). However, they allowed accurate estimations of the biomass-independent biodegradation parameters needed for model calculations. The concentration of dissolved ¹⁴CO₂ produced from ¹⁴C-pyrene was determined in parallel to fluorescence readings of suspensions prepared as described above and placed in 8-ml glass vials. The vials were maintained upright and without shaking to mimic the conditions of the fluorescence determinations. At certain time intervals, 0.5-ml samples were taken from the vials and analyzed for their ¹⁴CO₂ content. In some experiments, the aliquots were taken directly from the cuvette at the end of each experimental period. This volume was introduced into a 50-ml glass tube (Pyrex 8424) that had at the bottom 1 ml of an acidified (pH 2.3) solution of HgCl₂ (10 g/liter) to stop biodegradation and release ¹⁴CO₂ into the headspace. The tube was immediately closed with a Teflon-lined stopper, from which a vial of 1 ml containing 0.5 ml of 0.5 M NaOH was suspended to trap ¹⁴CO₂. The flasks were kept upright for at least 8 h at 23 ± 2°C on an orbital shaker operating at 100 rpm. This procedure allowed the complete recovery of the ¹⁴CO₂ initially present in the solution. The NaOH solution was then mixed with 5 ml of liquid scintillation cocktail (Ready Safe, Beckman Instruments, Fullerton, CA), and the mixture was kept in darkness for about 8 h to allow dissipation of chemiluminescence. Radioactivity was measured with a liquid scintillation counter. No significant losses of ¹⁴CO₂ were expected during biodegradation experiments, given the small headspace in the cuvette and its closure with a gas-tight cap. Mass balances performed after mineralization determinations accounted for 75 to 100% of the initial radioactivity present in the system. The bioavailable fraction of ¹⁴C-pyrene in the system, *f_{bio}*, was estimated in experiments with sediment suspensions according to the following equation:

$$f_{bio} = \frac{F_{min}}{F_{ef}} \quad (2)$$

where *F_{min}* is the extent of mineralization measured at the end of the experimental period when dissolved pyrene concentrations remained at constant levels and *F_{ef}* is the fractional extent of mineralization of pyrene, previously determined for *M. gilvum* VM552 to be 22.6% in the absence of sediment.

Model calculations. The kinetic analysis of the biodegradation experiments that separately examined oxygen and sorption limitations was integrated into model calculations predicting the concentration of aqueous-phase pyrene in sediment suspensions. For this purpose, the maximum rates of pyrene uptake at different oxygen concentrations were fitted by linear regression to the Lineweaver-Burk inverse form of the Michaelis-Menten equation:

$$\frac{1}{v} = \frac{K_{om}}{V_{max}} \times \frac{1}{[O_2]} + \frac{1}{V_{max}} \quad (3)$$

where *v* is the specific rate of uptake (in nanograms per microgram of protein per minute), [O₂] is the millimolar oxygen concentration, *V_{max}* is the maximum specific uptake rate under conditions of saturating air (in nanograms per microgram of protein per minute), and *K_{om}* is the oxygen concentration resulting in $v = 0.5(V_{max})$. According to this equation, a plot of 1/*v* versus 1/[O₂] yields a straight line with an intercept on the y axis of 1/*V_{max}* and a slope of *K_{om}*/*V_{max}*.

The half-saturation constant for pyrene, *K_{pm}*, corresponding, under conditions of air saturation, to the concentration of pyrene (in nanograms per milliliter) resulting in one-half of the maximum specific uptake rate, *V_{max}* (in nanograms per microgram of protein per minute), was calculated using the governing equation:

$$\frac{d[pyr]}{dt} = \frac{V_{max} \times P \times [pyr]}{K_{pm} + [pyr]} \quad (4)$$

where *P* is the concentration of protein (in micrograms of protein per milliliter). This has the following solution:

$$\ln \left[\frac{Pyr_t}{Pyr_0} \right] + Pyr_t - Pyr_0 = \frac{V_{max} \times P \times t}{K_{pm}} \quad (5)$$

where *Pyr₀* and *Pyr_t* are the aqueous concentrations of pyrene at time 0 and *t*,

respectively, and t is time (min). Replacement using the fluorescence values was calculated as follows:

$$P_{\text{Pyr}} = \frac{(flu_o - bkgd)}{rf} \quad (6)$$

where flu_o , $bkgd$, and rf are fluorescence readings, background fluorescence, and response factor, respectively; rearrangement gives the following equation:

$$\ln(flu_o - bkgd) + \frac{flu_o}{rf} = \frac{V_{\text{max}} \times P \times t}{K_{\text{pm}}} + \ln(flu_o - bkgd) + \frac{flu_o}{rf} \quad (7)$$

The value of K_{pm} was calculated from equation 7 by fitting values to fluorescence readings from biodegradation experiments after fixing the V_{max} value that was determined for uptake at different oxygen concentrations.

The results of biodegradation experiments in sediment suspensions were analyzed with the following differential equation:

$$\frac{d(pyr_w)}{dt} = -k_{\text{bio}} \times pyr_w + k_{\text{desorb}} \times \left(\frac{pyr_{\text{sed}}}{K_d - pyr_w} \right) \quad (8)$$

where pyr_w (in nanograms per milliliter) is the concentration of pyrene in the aqueous phase, t is time in minutes, k_{bio} (per minute) is the pseudo-first-order rate constant for biodegradation of dissolved pyrene, k_{desorb} is the first-order rate constant for desorption of pyrene (per minute), pyr_{sed} is the concentration of sorbed pyrene (in nanograms per gram), and K_d (in milliliters per gram) is the solid-water distribution coefficient. The integral form of this equation is as follows:

$$[pyr_w]_t = ([pyr_w]_0 - A) \times e^{-Bt} + A \quad (9)$$

with

$$A = \frac{k_{\text{desorb}} \times (pyr_{\text{sed}}/K_d)}{k_{\text{bio}} + k_{\text{desorb}}} \quad (10)$$

$$B = k_{\text{bio}} + k_{\text{desorb}} \quad (11)$$

For our modeling fits, we took A to represent the quasi-steady-state concentration of aqueous-phase pyrene achieved during long time spans when dissolved pyrene levels reflected a balance of desorption inputs and biodegradation removals, whereas B represents the sum of first-order rate constants for processes changing aqueous-phase pyrene concentrations. The values for A and B were obtained by the use of Microsoft Excel 2003 (Solver option) to minimize the differences in the cumulative squared residual values between experimental and calculated values of pyrene concentrations. These values were then used to calculate k_{desorb} by solving equations 10 and 11:

$$k_{\text{desorb}} = \frac{A \times B \times K_d}{pyr_{\text{sed}}} \quad (12)$$

The effect of oxygen- and sorption-limited biodegradation on the evolution of aqueous pyrene concentrations in sediment suspensions was simulated with equation 9 using the parameter values obtained experimentally in this study (V_{max} , K_{om} , K_{pm} , K_d , and k_{desorb}) or as previously published (K_d and k_{desorb} [2, 12, 26]). The first-order biodegradation rate constant from equation 9, k_{bio} (per minute), was adjusted for different oxygen concentrations according to the following equation:

$$k_{\text{bio}} = V_{\text{max}} P \times \frac{[O_2]}{K_{\text{om}} + [O_2]} \times \frac{1}{K_{\text{pm}} + [pyr]} \quad (13)$$

where P (in micrograms of protein per milliliter) is the biomass concentration operating at a certain oxygen concentration ($[O_2]$) and an initial aqueous pyrene concentration ($[pyr]$). The values for the empirical ratio of the pyrene concentration in the solid phase to that in the dissolved phase (Q_d) were calculated from the simulated aqueous concentrations by assuming that the solid-phase concentration remained constant.

RESULTS

Effects of induced, noninduced, and inactivated cells on aqueous-phase ^{14}C -pyrene. To test the use of synchronous fluorescence spectroscopy for following biodegradation of aqueous-phase ^{14}C -pyrene in bacterial and sediment suspen-

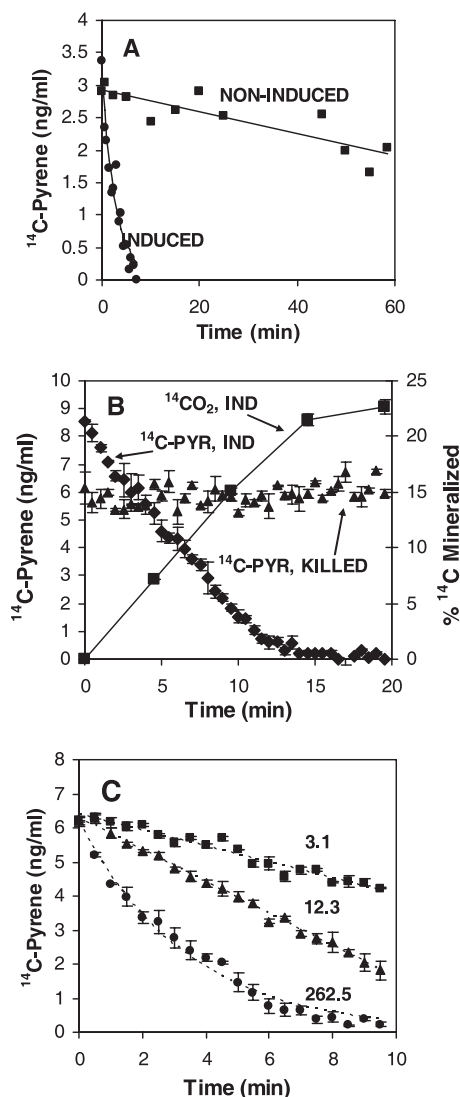


FIG. 1. (A) Time courses of dissolved ^{14}C -pyrene concentrations in the presence of noninduced cells of *Mycobacterium gilvum* VM552 cultivated in Luria broth medium and induced, pyrene-grown cells. (B) Time courses of ^{14}C -pyrene concentrations in the presence of induced cells (^{14}C -PYR, IND) and of induced cells previously treated with mercuric chloride (^{14}C -PYR, KILLED), and percentages of chemicals converted into $^{14}\text{CO}_2$ in the presence of induced cells ($^{14}\text{CO}_2$, IND). (C) Effect of oxygen concentrations (indicated in the figure as 3.1, 12.3, and 262.5 μM) on the biodegradation of dissolved ^{14}C -pyrene in suspensions of induced cells. Error bars in panels B and C represent 1 standard deviation of the results of duplicate measurements.

sions, we examined various simplified systems. When we used only pyrene-grown bacteria, the fluorescence data showed rapid and complete loss of the dissolved compound in air-saturated solutions, as evidenced by the decrease in fluorescence signal to undetectable levels (Fig. 1A). The experiments showed that uptake of the compound may be an inducible process, because losses during the first 10 min were small whereas longer incubations (up to 1 h) with LB-grown cells (at 7.3 μg protein/ml or an OD_{600} of 0.019) produced decreases in aqueous-phase ^{14}C -pyrene levels (Fig. 1A); however, this slow

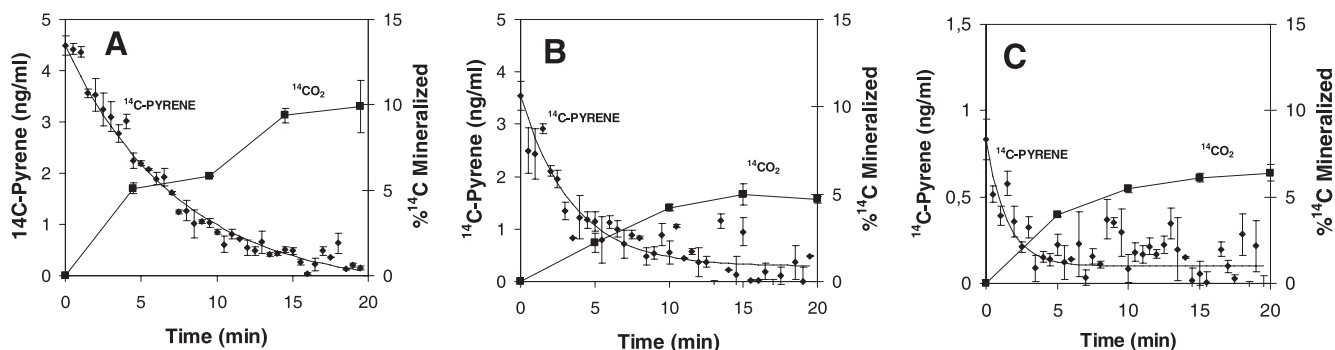


FIG. 2. Time course of ^{14}C -pyrene fluorescence and mineralization in suspensions of NQB sediment (from North Quincy Bay, Boston Harbor, Boston, MA) and NQB-BC sediment (NQB sediment amended with soot at 1% [wt/wt]) previously equilibrated with ^{14}C -pyrene solutions and inoculated with *Mycobacterium gilvum* VM552. The solid line represents the predictions from equation 9. Conditions (referring to sediment and PAH initial concentrations): (A) NQB at 400 mg/liter, 8.4 ng/ml ^{14}C -pyrene; (B) NQB at 1,600 mg/liter, 15.1 ng/ml ^{14}C -pyrene; (C) NQB-BC at 400 mg/liter, 8.4 ng/ml ^{14}C -pyrene. Error bars represent 1 standard deviation.

uptake may also have reflected some passive uptake from solution into the cells. Measurement of evolved $^{14}\text{CO}_2$ showed that uptake of ^{14}C -pyrene by induced bacteria was strongly coupled to its mineralization (Fig. 1B). Noninduced cells were not able to mineralize the chemical under these conditions. The extent of mineralization reached after complete consumption of the aqueous-phase compound was within the expected values for mineralization of PAHs. We did not observe any compound disappearance when induced bacterial suspensions were treated with mercuric chloride 5 min before the assay (Fig. 1B), indicating that passive sorption onto bacterial cells was not significantly increased in induced cells. Mineralization of the chemical by these inactivated cells was negligible (<1%).

Effect of oxygen concentration on uptake of ^{14}C -pyrene. Oxygen concentrations had a strong effect on the biodegradation of aqueous-phase ^{14}C -pyrene by induced cells (Fig. 1C). For low oxygen concentrations, the disappearance of this PAH was slow and represented a nearly zero-order reaction with respect to the ^{14}C -pyrene concentration, occurring at constant rates of 0.064 ± 0.002 and 0.130 ± 0.006 ng μg protein $^{-1}$ min $^{-1}$ at 3.1 and 12.3 μM oxygen concentrations, respectively. Under conditions of air saturation (262.5 μM), ^{14}C -pyrene loss occurred at a rate of 0.385 ± 0.065 ng μg protein $^{-1}$ min $^{-1}$ during the first 2 min and decreased with time. The fractions of substrate transformed to $^{14}\text{CO}_2$ at the end of the experimental period (9.5 min) were $7.0 \pm 1.9\%$, $10.2 \pm 2.0\%$, and $28.2 \pm 5.5\%$ at 3.1 μM , 12.3 μM , and 262.5 μM oxygen, respectively. Uptake of ^{14}C -pyrene also occurred in suspensions of pyrene-grown cells containing no measurable oxygen, although at a rate (0.035 ± 0.007 ng μg protein $^{-1}$ min $^{-1}$) much slower than that measured at known oxygen concentrations. Linear regression ($R^2 > 0.96$) of equation 3 with the maximum rates of compound uptake occurring at five different oxygen concentrations (3.1, 6.2, 12.3, 18.5, and 262.5 μM) resulted in a V_{max} value of 0.34 ng μg protein $^{-1}$ min $^{-1}$ and a K_{om} of 14.1 μM . The pyrene half-saturation constant, K_{pm} , was calculated from equation 7 with the data from the ^{14}C -pyrene uptake determination (Fig. 1B) and the previously determined value of V_{max} . The value obtained for K_{pm} was 1.23 ± 0.14 ng/ml (6.04 ± 0.68 nM).

Effect of sorption to black carbon on biodegradation of ^{14}C -pyrene. A previous study, performed with untreated and combusted NQB sediment, showed the strong contribution of black carbon to the overall sorption of pyrene in this sediment (1). We enriched this sample in BC by adding diesel soot (1% by weight). This sample is referred to here as NQB-BC. Sorption kinetics experiments showed that, at a solid-phase/water-phase ratio of 400 mg/liter, the dissolved ^{14}C -pyrene concentrations approached equilibrium, with half-lives of about 20 h and <6 h for the NQB and NQB-BC sediments, respectively (data not shown). K_d values were estimated by assuming that the dissolved ^{14}C -pyrene concentrations observed after 200 h reflected sorption equilibria. Not surprisingly, the NQB-BC sample exhibited an enhanced sorption capacity due to the addition of the diesel soot. The log K_d values estimated for NQB and NQB-BC sediments were 3.38 ± 0.04 and 4.09 ± 0.04 , respectively. The former was close to, but lower than, the value previously reported with this sediment, 3.72 ± 0.17 (1), presumably because the sorptive equilibrium for this system was not fully reached even at 200 h (20).

The addition of pyrene-grown cells to these sediment suspensions caused the fast decrease of the pyrene fluorescence signal and a simultaneous transformation of the compound into $^{14}\text{CO}_2$ (Fig. 2). The bioavailable fraction of pyrene in the system (f_{bio}), as evidenced by the ratio of $^{14}\text{CO}_2$ formed at the end of the 20-min experimental period compared to the corresponding sediment-free results, was lower than 1.0 for all sediment suspensions (Table 1), indicating the impact of sorption on biodegradation. Furthermore, sorption to diesel soot was clearly the cause for diminished mineralization of pyrene in NQB-BC suspensions, given that the observed f_{bio} value was lower than that seen with NQB at the same sediment concentration (400 mg/liter). In addition, f_{bio} values were very close to the corresponding aqueous fraction of pyrene at equilibrium, supporting the assumption of constant concentrations of pyrene in the sediment underlying equation 9. Indeed, the concentration of aqueous-phase pyrene changed during biodegradation in accordance with that equation (Fig. 2), indicating that the concentration of aqueous-phase pyrene (pyr_w) during active biodegradation was dependent on the simultaneous net

TABLE 1. Effect of sorption to sediments on biodegradation of aqueous-phase pyrene by *Mycobacterium gilvum* VM552

Sediment ^a	r_{sw}^b (mg/liter)	f_{bio}^c	pyr_w^d (ng/ml)		B^e ($k_{bio} + k_{desorb}$) (min^{-1})	k_{desorb}^f (min^{-1})
			Initial	Steady state		
NOB	400	0.43 ± 0.13	4.49 ± 0.39	0.30 ± 0.09^g	0.135 ± 0.012	0.0096 ± 0.0037
	800	0.36 ± 0.03	3.49 ± 0.04	0.23 ± 0.04^g	0.115 ± 0.030	0.0064 ± 0.0028
	1,600	0.21 ± 0.02	3.55 ± 0.56	0.29 ± 0.09^h	0.288 ± 0.007	0.0254 ± 0.0085
NOB-BC	400	0.28 ± 0.04	0.84 ± 0.23	0.15 ± 0.02^h	0.684 ± 0.146	0.0683 ± 0.0021

^a NO, North Quincy Bay in Boston Harbor, Boston, MA; NOB-BC, NOB sediment amended with 1% diesel soot.

^b r_{sw} , solid-phase/water-phase ratio.

^c f_{bio} , bioavailable fraction.

^d pyr_w , dissolved concentration of pyrene (total concentration, 8.40 ng/ml) at equilibrium before the addition of bacteria (Initial) and at the end of the biodegradation experiments (Steady state). The treatment with NOB at 1,600 mg/liter initially contained 15.10 ng/ml total pyrene.

^e B , first-order rate constant for dissipation of aqueous-phase pyrene (calculated with curve fitting equation 9).

^f k_{desorb} , rate constant for desorption of pyrene (calculated with equation 12).

^g Mean \pm standard deviation of experimental values during the last 5 min of incubation.

^h Value for A (quasi-steady-state concentration of aqueous-phase pyrene; see Materials and Methods) \pm standard deviation (obtained by curve fitting equation 9).

desorption of the compound from the sediment. Furthermore, Fig. 2B and C show that equation 9 satisfactorily predicts the maintenance of steady-state concentrations of dissolved pyrene during slow (but significant) $^{14}CO_2$ production. The kinetic analysis (Table 1) showed higher B values for higher r_{sw} values and with NOB-BC; while some of this trend can be explained by larger concentrations of solid leading to a faster system approach to sorptive equilibration (34), most of the increase (contrast B and k_{desorb} in Table 1) was due to higher k_{bio} values at lower aqueous-phase concentrations of pyrene resulting from the nonlinear nature of equation 13.

Integrating the effects of oxygen limitation and sorption on the biodegradation of pyrene. In order to assess the combined impacts of limited oxygen and sorptive interactions on the biodegradation of pyrene, simulations were performed to evaluate the removal of pyrene at different oxygen concentrations in initially equilibrated sediment/water systems. Model predictions performed with equation 9 for biodegradation in suspensions of NOB sediment at 1,600 mg/liter (Fig. 3A) show that oxygen tensions at or above the experimentally determined value of K_{om} (14.1 μM) should cause decreases in the aqueous concentrations of pyrene similar to those seen under air-saturated conditions (i.e., down to less than 1 ng/ml). Even at sub- K_{om} levels of oxygen, losses due to biodegradation were expected to be significant. For example, at 5 μM oxygen, biodegradation-desorption modeling causes the quasi-steady-state aqueous concentration to be about 1.3 ng/ml (Fig. 3A). If this type of result were applicable to surface sediment layers that are microaerobic, then one would see an important impact on "field-derived" $\log Q_d$ values (i.e., observed ratios of sorbed-to-dissolved compounds that may deviate from sorption equilibrium ratios, or K_d values, because biotransformation is too fast to allow sorptive equilibration). For example, the same sediment (initial $\log Q_d$ of 3.38) with oxygen-saturated pore water would exhibit a $\log Q_d$ of 4.17 whereas that seen with 5 $\mu M O_2$ would have a $\log Q_d$ of 3.76.

Further modeling was performed to ascertain whether oxygen-limited plus desorption-limited biodegradation could feasibly explain previously reported field conditions (Fig. 3B). The scenario considered repeated short-term resuspension events causing a solids content of 1,600 mg/liter, with sediment properties typical of parts of Boston Harbor (off Spectacle Island;

native pyrene concentration of 1.1 mg/kg, an OC content of 4.0%, and a BC content of 0.3% [2, 26]). Previous measures of the pyrene in this bed sediment and its pore water showed a $\log K_d$ value for pyrene sorption of 5.2, a value that was approximately 1 logarithm unit greater than expected, according to the

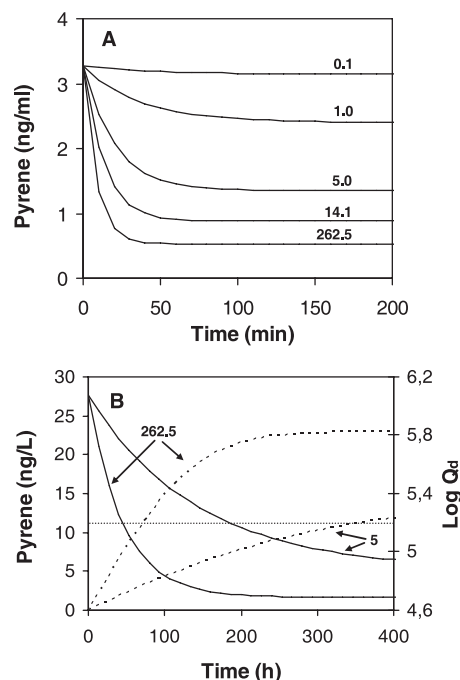


FIG. 3. Model predictions of pyrene aqueous concentrations and empirical distribution ratio ($\log Q_d$) in sediment suspensions with biodegradation operating at different oxygen tensions. (A) Effect of oxygen concentrations (indicated in the figure as 0.1, 1.0, 5.0, 14.1, and 262.5 μM) on the evolution of dissolved pyrene in suspensions of NOB (sediment from North Quincy Bay in Boston Harbor, Boston, MA) under experimental conditions corresponding to those described for Fig. 2B. (B) Evolution of aqueous-phase pyrene (solid curves) and $\log Q_d$ (dashed curves) at two different oxygen concentrations (5 and 262.5 μM) in suspensions of Spectacle Island sediment from Boston Harbor (2, 26) at a cell density of 10^3 cells/ml (see text for a description of the other simulation conditions). The dotted horizontal line indicates the field-estimated $\log K_d$ value (2). Note the different scale units on the left side of panels A and B.

OC content of the sediments (26). Black-carbon-based model predictions did not completely explain the enhanced sorption, as they still underestimated $\log K_d$ values by 0.6 logarithm units in the upper zone of the sediments, which is subject to bioturbation (2). To assess whether oxygen-limited and desorption-limited biodegradation could account for these differences, we took the BC-predicted $\log K_d$ value of 4.6 for our modeling (i.e., $K_d = 0.003 \cdot 10^{6.25} \cdot \text{pyrene}^{-0.38}$, assuming that the dissolved pyrene level was $0.004 \mu\text{g/liter}$ [1]). Because a value for the desorption rate constant was not available for this sediment, and considering that more than 95% of native pyrene is usually found in sediments in the very slowly desorbing fraction, we took a value of $1.31 \times 10^{-3} \text{ h}^{-1}$ for this constant (12). The density of pyrene-degrading cells was taken as 10^3 cells/ml. This relatively low cell number was based on estimations of numbers of phenanthrene-degrading bacteria in sediments (up to 10^7 cells/g of sediment [9]), considering that the number of pyrene degraders in the water column was due exclusively to the input of the resuspended sediment particles and that naturally occurring populations of pyrene-degrading microorganisms are usually 1/10 the size of phenanthrene-degrading populations (19). Model predictions under these conditions showed that biodegradation operating at very low oxygen tensions ($5 \mu\text{M}$) was still able to significantly reduce the concentration of aqueous-phase pyrene (Fig. 3B)—15 days being needed to drive the $\log Q_d$ value to the field-observed value of $\log K_d$.

DISCUSSION

The new method for continuous measurement of ^{14}C -pyrene uptake by *Mycobacterium gilvum* VM552 was a useful means to characterize kinetically the biodegradation of aqueous-phase pyrene at different oxygen concentrations under different sorption conditions. However, in our experimental system, cells that were left uninduced with respect to pyrene metabolism, and induced cells incubated at a concentration resulting in no detectable oxygen, also caused losses of pyrene in solution. This was expected, because the amount of biomass used in the assays was sufficient to passively sorb a significant fraction of the compound, taking into account the amount of organic carbon (OC) present in the system as bacterial cell components and the $\log K_{oc}$ of pyrene, which is 4.7 (1). For example, approximately 40% of the compound would be expected to sorb onto cells added at $7.30 \mu\text{g protein/ml}$ or $15 \text{ mg of OC/liter}$ (one cell of *M. gilvum* VM552 contained approximately $1.4 \text{ pg of protein}$ and 2.8 pg of C , assuming that cell protein contains 50% of cell C).

The low bacterial cell densities used in the present work resulted in passive sorption to the cells that was reduced compared to the level that was found in previous studies reporting nearly instantaneous sorption of PAH to bacterial cells and dissolved humic materials, with equilibration times of less than 1 min (3, 8, 27). This lower rate of passive sorption allowed us to observe profound differences between induced and uninduced cells in uptake rates. Therefore, we believe that the biodegradation-driven uptake overwhelmed the low rate of spontaneous sorption to bacterial cells in our degradation testing, given our experimental conditions. The precise mechanism is unknown, but it may involve a specific, energy-dependent

mechanism for substrate uptake by induced cells, in addition to passive diffusion (27).

The observed shift in biodegradation kinetics under conditions ranging from high to low oxygen concentrations (Fig. 1C) is consistent with the existence of an energy-dependent mechanism for pyrene uptake. It is possible that, at limiting oxygen concentrations, this mechanism was inhibited. A similar effect has been described for two inhibitors of active transport (cyanide and carbonyl cyanide *m*-chlorophenylhydrazone), which prevented active uptake of phenanthrene by induced cells of *Mycobacterium* sp. RJII-135 but not uptake by passive diffusion (27). It is possible, therefore, that the linear kinetics observed in our study at low oxygen tensions may be a reflection of the uptake of the compound by passive diffusion, whereas an active acquisition contributed to the first-order uptake observed for air-saturated conditions. Another possible explanation for the enhanced uptake by induced bacteria is that the active consumption of pyrene due to biodegradation caused steepened concentration gradients through the unstirred boundary layer (UBL) surrounding the cells, resulting in an enhanced diffusional flux toward the cells. Such a UBL, containing much lower substrate concentrations than the surrounding media, is usually formed around bacteria as a result of differences in the rates of uptake and the rates of diffusion through the UBL (16, 29).

The results shown here indicate that, under the bioavailability restrictions imposed by strong sorption (e.g., to BC), an active population of degrading cells drove the aqueous concentration of pyrene to a steady-state level caused by desorption inputs and biodegradation removals. Model calculations further indicate that oxygen tensions far below saturation levels in water were sufficient to allow steady-state concentrations similar to those appearing in air-saturated conditions. The oxygen concentration affected sorption-limited biodegradation only below a threshold value, as determined by K_{om} . To our knowledge, the value found for K_{om} ($14.1 \mu\text{M}$) is the first estimation of a K_{om} value for pyrene uptake by microorganisms. This value is slightly higher than the K_{om} value determined for growth on pyrene of a *Mycobacterium* sp. strain ($5.9 \mu\text{M}$) (7) and is close to that found for naphthalene uptake by *Pseudomonas putida* G7 ($15.6 \mu\text{M}$) (21). These observations suggest that very low oxygen inputs are needed for the aerobic transformation of PAHs present in BC-containing sediments subject to resuspension events or bioturbation activity, provided that they harbor an active, aerobic population of PAH-degrading bacteria. The existence of such a potential for aerobic biodegradation is plausible, considering that faunal activity may introduce up to $100 \mu\text{M}$ dissolved oxygen into deeper sediment layers by burrowing and irrigation (11), and surface and burrow sediments have been identified as the main compartments for aerobic mineralization of pyrene in marine sediments compared with reduced bulk sediment (13). However, the simultaneous occurrence of other carbon sources and/or other organisms competing for oxygen should also be considered in future works addressing the actual relevance of oxygen-limited aerobic biodegradation of PAHs sorbed to BC-containing sediments. This concept complements recent studies showing the significant contribution of anaerobic, sulfate-dependent biodegradation to the dissipation of PAHs in anoxic sediments (30, 33). Recent research has also demonstrated a

substantial role of black carbon regarding enhanced sorption observations in sediments (2, 26), and our study extends those findings by suggesting that aerobic biodegradation may also contribute to sorption enhancements observed *in situ*.

ACKNOWLEDGMENTS

Support for this research was provided by the European Union (contract EVK1-CT-2001-00101), the Spanish Ministry of Science and Innovation (VEM2004-08556, CGL2007-64199/BOS, and Mobility Program for Visiting Scientists), and the U.S. National Science Foundation (NSF grant BES 0607136).

We thank John MacFarlane for technical assistance.

REFERENCES

- Accardi-Dey, A., and P. M. Gschwend. 2002. Assessing the combined roles of natural organic matter and black carbon as sorbents in sediments. *Environ. Sci. Technol.* **36**:21–29.
- Accardi-Dey, A., and P. M. Gschwend. 2003. Reinterpreting literature sorption data considering both absorption into organic carbon and adsorption onto black carbon. *Environ. Sci. Technol.* **37**:99–106.
- Backhus, D. A., and P. M. Gschwend. 1990. Fluorescent polycyclic aromatic hydrocarbons as probes for studying the impact of colloids on pollutant transport in groundwater. *Environ. Sci. Technol.* **24**:1214–1223.
- Berardesco, G., S. Dyhrman, E. Gallagher, and M. Shiaris. 1998. Spatial and temporal variation of phenanthrene-degrading bacteria in intertidal sediments. *Appl. Environ. Microbiol.* **64**:2560–2565.
- Boyd, T. J., M. T. Montgomery, K. J. Steele, J. W. Pohlman, S. R. Reatherford, B. J. Spargo, and D. C. Smith. 2005. Dissolved oxygen saturation controls PAH biodegradation in freshwater estuary sediments. *Microb. Ecol.* **49**:226–235.
- Daniels, L., R. S. Handson, and J. A. Philips. 1994. Chemical analysis, p. 512–554. *In* A. P. Gerhardt, R. G. E. Murray, W. A. Wood, and N. R. Krieg (ed.), *Methods for general and molecular bacteriology*. ASM Press, Washington, DC.
- Fritzsche, C. 1994. Degradation of pyrene at low defined oxygen concentrations by a *Mycobacterium* sp. *Appl. Environ. Microbiol.* **60**:1687–1689.
- Gauthier, T. D., E. C. Shane, W. F. Guerin, W. R. Seltz, and C. L. Grant. 1986. Fluorescence quenching method for determining constants for polycyclic aromatic hydrocarbons binding to dissolved humic materials. *Environ. Sci. Technol.* **20**:1162–1166.
- Geiselbrecht, A. D., R. P. Herwig, J. W. Deming, and J. T. Staley. 1996. Enumeration and phylogenetic analysis of polycyclic aromatic hydrocarbon-degrading marine bacteria from Puget Sound sediments. *Appl. Environ. Microbiol.* **62**:3344–3349.
- Ghosh, U., J. R. Zimmerman, and R. G. Luthy. 2003. PCB and PAH speciation among particle types in contaminated harbor sediments and effects on PAH bioavailability. *Environ. Sci. Technol.* **37**:2209–2217.
- Glud, R. N., J. K. Gundersen, H. Roy, and B. B. Jorgensen. 2003. Seasonal dynamics of benthic O₂ uptake in a semienclosed bay: importance of diffusion and faunal activity. *Limnol. Oceanogr.* **48**:1265–1276.
- Gomez-Lahoz, C., and J. J. Ortega-Calvo. 2005. Effect of slow desorption on the kinetics of biodegradation of polycyclic aromatic hydrocarbons. *Environ. Sci. Technol.* **39**:8776–8783.
- Granberg, M. E., R. Hansen, and H. Selck. 2005. Relative importance of macrofaunal burrows for the microbial mineralization of pyrene in marine sediments: impact of macrofaunal species and organic matter quality. *Mar. Ecol. Prog. Ser.* **288**:59–74.
- Guerin, W. F., and S. A. Boyd. 1997. Bioavailability of naphthalene associated with natural and synthetic sorbents. *Water Res.* **31**:1504–1512.
- Gustafsson, Ö., F. Haghseta, J. Chan, J. MacFarlane, and P. M. Gschwend. 1997. Quantification of the dilute sedimentary soot phase: implications for PAH speciation and bioavailability. *Environ. Sci. Technol.* **31**:203–209.
- Haftka, J. J. H., J. R. Parsons, H. A. J. Govers, and J. J. Ortega-Calvo. 2008. Enhanced kinetics of solid-phase microextraction and biodegradation of polycyclic aromatic hydrocarbons in the presence of dissolved organic matter. *Environ. Toxicol. Chem.* **27**:1526–1532.
- Hurst, C. J., R. C. Sims, J. L. Sims, D. L. Sorensen, J. E. McLean, and S. Huling. 1996. Polycyclic aromatic hydrocarbons biodegradation as a function of oxygen tension in contaminated soil. *J. Hazard. Mater.* **51**:193–208.
- Johnsen, A. R., J. R. de Liphay, S. J. Sorensen, F. Ekelund, P. Christensen, O. Andersen, U. Karlson, and C. S. Jacobsen. 2006. Microbial degradation of street dust polycyclic aromatic hydrocarbons in microcosms simulating diffuse pollution of urban soil. *Environ. Microbiol.* **8**:535–545.
- Johnsen, A. R., and U. Karlson. 2005. PAH degradation capacity of soil microbial communities—does it depend on PAH exposure? *Microb. Ecol.* **50**:488–495.
- Kuo, D. T. F., R. G. Adams, S. M. Rudnick, R. F. Chen, and P. M. Gschwend. 2007. Investigating desorption of native pyrene from sediment on minute- to month-timescales by time-gated fluorescence spectroscopy. *Environ. Sci. Technol.* **41**:7752–7758.
- Law, A. M. J., and M. D. Aitken. 2006. The effect of oxygen on chemotaxis to naphthalene by *Pseudomonas putida* G7. *Biotechnol. Bioeng.* **93**:457–464.
- LeBlanc, L. A., J. D. Gulnick, B. J. Brownawell, and G. T. Taylor. 2006. The influence of sediment resuspension on the degradation of phenanthrene in flow-through microcosms. *Mar. Environ. Res.* **61**:202–223.
- Lohmann, R., R. M. Burgess, M. G. Cantwell, S. A. Ryba, J. K. MacFarlane, and P. M. Gschwend. 2004. Dependency of polychlorinated biphenyl and polycyclic aromatic hydrocarbon bioaccumulation in *Mya arenaria* on both water column and sediment bed chemical activities. *Environ. Toxicol. Chem.* **23**:2551–2562.
- Lohmann, R., J. MacFarlane, and P. M. Gschwend. 2005. Importance of black carbon to sorption of native PAHs, PCBs, and PCDDs in Boston and New York Harbor sediments. *Environ. Sci. Technol.* **39**:141–148.
- Maruya, K. A., R. W. Risenbrough, and A. J. Horne. 1996. Partitioning of polynuclear aromatic hydrocarbons between sediments from San Francisco Bay and their porewaters. *Environ. Sci. Technol.* **30**:2942–2947.
- McGroddy, S. E., and J. W. Farrington. 1995. Sediment porewater partitioning of polycyclic aromatic hydrocarbons in three cores from Boston Harbor, Massachusetts. *Environ. Sci. Technol.* **29**:1542–1550.
- Miyata, N., K. Iwahori, J. M. Foght, and M. R. Gray. 2004. Saturable, energy dependent uptake of phenanthrene in aqueous phase by *Mycobacterium* sp. strain RJGII-135. *Appl. Environ. Microbiol.* **70**:363–369.
- Ortega-Calvo, J. J., and M. Alexander. 1994. Roles of bacterial attachment and spontaneous partitioning in the biodegradation of naphthalene initially present in nonaqueous-phase liquids. *Appl. Environ. Microbiol.* **60**:2643–2646.
- Ortega-Calvo, J. J., and C. Saiz-Jimenez. 1998. Effect of humic fractions and clay on biodegradation of phenanthrene by a *Pseudomonas fluorescens* strain isolated from soil. *Appl. Environ. Microbiol.* **64**:3123–3126.
- Quantin, C., E. J. Joner, J. M. Portal, and J. Berthelin. 2005. PAH dissipation in a contaminated river sediment under oxic and anoxic conditions. *Environ. Pollut.* **134**:315–322.
- Reichenberg, F., and P. Mayer. 2006. Two complementary sides of bioavailability: accessibility and chemical activity of organic contaminants in sediments and soils. *Environ. Toxicol. Chem.* **25**:1239–1245.
- Rhodes, A. H., A. Carlin, and K. T. Semple. 2008. Impact of black carbon on the extraction and mineralization of phenanthrene in soil. *Environ. Sci. Technol.* **42**:740–745.
- Rothermich, M. M., L. A. Hayes, and D. R. Lovley. 2002. Anaerobic, sulfate-dependent degradation of polycyclic aromatic hydrocarbons in petroleum-contaminated harbor sediment. *Environ. Sci. Technol.* **36**:4811–4817.
- Schwarzenbach, R. P., P. M. Gschwend, and D. M. Imboden. 2003. *Environmental organic chemistry*, 2nd ed. John Wiley & Sons Inc., Hoboken, NJ.
- Vila, J., Z. Lopez, J. Sabate, C. Minguillon, A. M. Solanas, and M. Grifoll. 2001. Identification of novel metabolite in the degradation of pyrene by *Mycobacterium* sp. strain AP1: actions of the isolate on two and three ring polycyclic aromatic hydrocarbons. *Appl. Environ. Microbiol.* **67**:5497–5505.
- Vo-Dinh, T. 1981. Synchronous excitation spectroscopy, p. 167–192. *In* E. L. Wehry (ed.), *Modern fluorescence spectroscopy*. Plenum Press, New York, NY.
- Yang, Z. F., J. L. Feng, J. F. Niu, and Z. Y. Shen. 2008. Release of polycyclic aromatic hydrocarbons from Yangtze River sediment cores during periods of simulated resuspension. *Environ. Pollut.* **155**:366–374.